

WHERE'S THE COMPRESSION? EXPLAINING THE LACK OF CONTRACTIONAL STRUCTURES ON ICY SATELLITES. Robert T. Pappalardo¹ and Daniel M. Davis², ¹Jet Propulsion Laboratory, California Institute of Technology, Mail Stop 183-301, Pasadena, CA 91109, ²Stony Brook University, Department of Geosciences, Stony Brook, NY 11794-3357.

Introduction: A longstanding question in outer planet satellite geology is: Where's the compression? Icy satellites are rich in structures interpreted as extensional-tectonic, most commonly from normal faulting [1-7]. Lanes of normal fault blocks on icy satellites can represent 10s of percent local extensional strain [4,7], but complementary contractional structures are rare. On Earth and the other terrestrial planets, contractional structures are dominated by reverse faults, most commonly as sets of thrust blocks [8]. To date, thrust blocks have been inferred only on the relatively small icy satellites, notably Dione [9] and Enceladus [10].

Here we consider issues of contractional structures on icy satellites, concluding that it is not surprising for such structures to be relatively rare, especially on larger satellites. Relevant issues include: 1) for a given vertical (overburden) stress, the differential stress required for contractional (reverse) brittle-frictional faulting is considerably greater than for extensional (normal) faulting, 2) extension leads to increased thermal gradients, so compressed regions tend to be stronger (cooler) than warmer (weaker) extended zones, 3) a very weak warm ice substrate allows contracting regions to be very broad, allowing them to accommodate large amounts of strain through creep at depth; and 4) significantly greater stress is required for brittle failure on higher gravity satellites.

Strength Envelopes: Fig. 1 illustrates the comparative lithospheric strength (absolute differential stress necessary for failure) as a function of depth, for several icy satellites with a range of surface gravities g (Ganymede, Europa, Dione, and Enceladus). Straight lines illustrate the failure strength of the pre-fractured (frictionally controlled) brittle lithosphere, assuming a friction coefficient $\mu_f = 0.69$ for pre-fractured ice with negligible cohesion [11]. Solid lines represent horizontal compression (least principal stress oriented vertically, $\sigma_3 = \rho g z$), and dashed lines are for horizontal extension (greatest principal stress oriented vertically, $\sigma_1 = \rho g z$), for lithospheric density $\rho = 1000 \text{ kg m}^{-3}$. Satellite gravity significantly affects the slope of the frictional failure line. Curves of Fig. 1 illustrate the failure strength of the ductile lower lithosphere for thermal gradients of 20 K km^{-1} and 40 K km^{-1} , and strain rates of 10^{-16} , 10^{-15} , and 10^{-14} s^{-1} . The ductile B rheology of [12] is adopted, assuming a surface temperature of 70 K (appropriate for higher latitudes on the jovian satellites, and lower latitudes on the saturnian satellites).

Lithospheric Failure Strength: It is well known that lithospheric strength is several times greater in compression than in extension. On Fig. 1, maximum lithospheric strength is approximated by the intersection of the brittle and ductile failure curves. Ganymede's lithosphere is ~ 3 times stronger in compression than in extension, for the same thermal gradient and strain rate. Ganymede's extensional-tectonic grooved

terrain [13] occurs in lanes typically 10s km wide representing extensional strains of 10s of percent [7], and lanes presumably formed sequentially in time. Extension is expected to create locally increased thermal gradients [14], with $\sim 40 \text{ K km}^{-1}$ appropriate to the formation of Ganymede's grooved terrain [13]. This thermal gradient implies a maximum lithospheric strength of $\sim 2 \text{ MPa}$ in extension. The extensional strain of any individual lane suggests compensation by compression elsewhere across Ganymede (unless the satellite expanded significantly during grooved terrain formation [15]). Thermal gradients in Ganymede's relatively broad, undeformed dark terrain were likely $< 20 \text{ K km}^{-1}$ [13], suggesting lithospheric strength $\sim 11 \text{ MPa}$. The tendency for greater strength in compression, combined with an expected lesser thermal gradient in contracted terrains, implies that >5 times as much compressional stress is required to produce reverse faults on Ganymede compared to the extensional stress necessary to form grooved terrain normal faults. Analogous results are implied for Europa, which has a similar gravity (albeit different thermal gradients).

For small Enceladus, $\sim 0.2 \text{ MPa}$ differential stress permits frictional failure in extension, for a thermal gradient of 40 K km^{-1} . Analogous to Ganymede, ~ 6 times greater stress is necessary for reverse faulting in compression compared to the stress extension if the thermal gradient in contracted terrains is reduced by half. Nevertheless, the $\sim 1.2 \text{ MPa}$ stress required for reverse faulting of cool Enceladean lithosphere is relatively modest. For Dione, about twice the stress is required for failure as compared to Enceladus.

Discussion: It is difficult for an icy satellite lithosphere to fail brittlely in compression, so contractional strain must be absorbed in other ways. As suggested for the lunar megaregolith, some contractional strain can be accommodated by compaction of fracture porosity within the shallow brittle lithosphere [16, 17] and will not be apparent at the surface. At depth, porosity is reduced by pressure and temperature [18]. Where porosity has been reduced to negligible amounts, lithospheric thickening will occur instead, producing only modest topography. (Long-wavelength mullion-like structures on Europa [19,20] may be an expression of such thickening.) The thickened root will reach beneath the brittle-ductile transition, and can relax through viscous flow.

In the ductile lower lithosphere, creep occurs readily in response to compression. A warm ice substrate is very weak, without substantial basal tractions, so the compensating contracting region can be very broad [21]. Because brittle failure strength in compression is significantly greater than in extension, compression creep can proceed at greater differential stresses without inducing brittle failure; thus, the creeping strain rate in contracted regions can be significantly higher

(by 1-2 orders of magnitude) than in extended regions. Combined with the greater areal extent of contracted terrains, ~2 to 3 orders of magnitude greater creep can be accommodated compared to extended regions.

Moreover, compared to the strain rate in extended terrains, strain rate is expected to be less in the broad regions accommodating compression. While extensional strain creates localized deformation (as in Ganymede's grooved terrain), compression can be distributed across a surrounding region that is perhaps an order of magnitude greater in lateral extent; thus, compressional strain rate would be an order of magnitude less than in extension. This means that the brittle lithosphere is slightly thinner and weaker in contracted regions than might otherwise be expected, and a slightly thicker region of ductile lithosphere exists be-

low such a region. The detailed implications of contractional creep require consideration of the grain-size sensitive creep of ice [22].

Conclusions: Sources of compressional stress sufficient for reverse faulting probably do not exist on most icy satellites. Instead, compression may result in porosity compaction within the upper brittle lithosphere, and thickening and creep in deeper, warmer regions. Contracted areas can be much broader than extended areas, so can experience greater creeping strain rates and accommodate significantly more creep. Geologically active small satellites are most likely to experience reverse faulting, as stress levels required to initiate compressional failure are relatively small. This is consistent with the inferred presence of thrust blocks on Dione and Enceladus, but not on Ganymede.

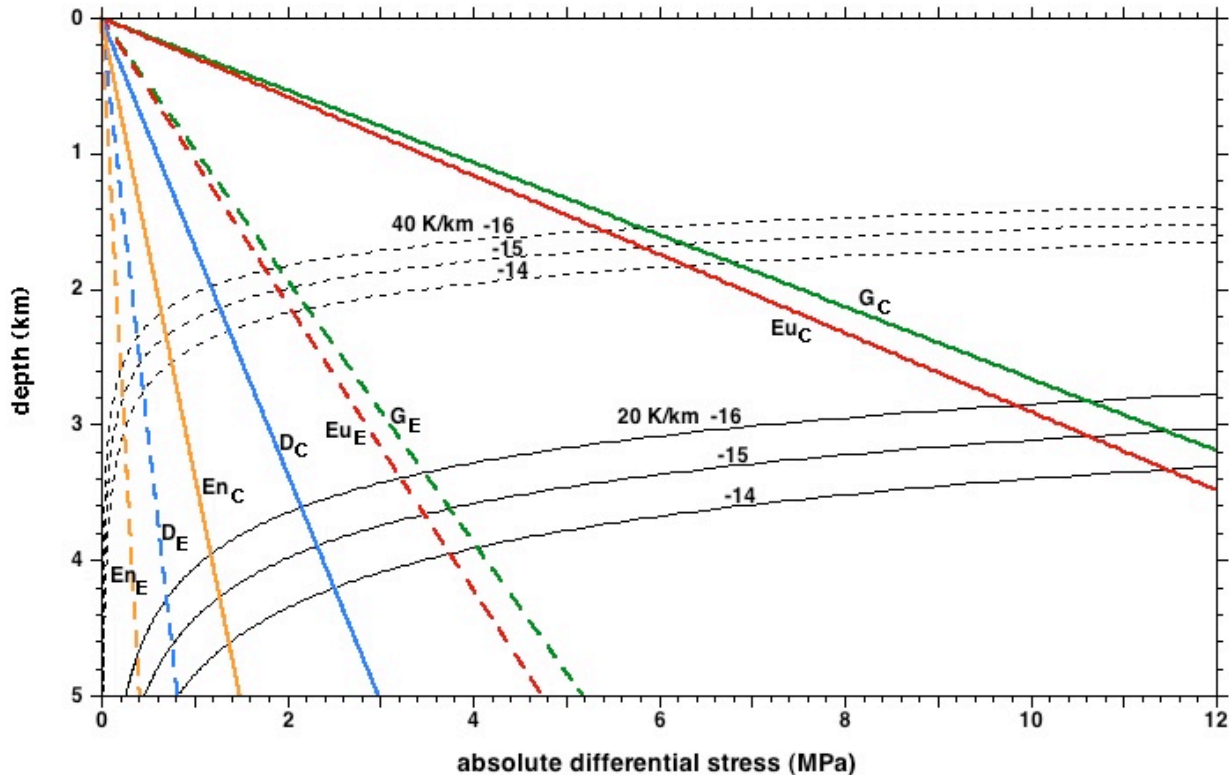


Figure 1. Icy satellite lithospheric strength in the brittle and ductile regimes, for representative satellite gravities, strain rates, and thermal gradients. G = Ganymede (green, $g = 1.43 \text{ m s}^{-2}$); Eu = Europa (red, $g = 1.31 \text{ m s}^{-2}$); D = Dione (blue, $g = 0.227 \text{ m s}^{-2}$); and En = Enceladus (gold, $g = 0.113 \text{ m s}^{-2}$). For the brittle failure lines, subscript C implies compression (solid straight lines), and subscript E implies extension (dashed straight lines). Ductile strength curves for ice use the ductile B regime of [12], a surface temperature of 70 K, and thermal gradients of 20 K km^{-1} (solid curves) and 40 K km^{-1} (dashed curves), as labeled with the log of strain rate ($10^{-16}, 10^{-15}, \text{ and } 10^{-14} \text{ s}^{-1}$).

References: [1] Squyres & Croft (1986), in *Satellites*, pp. 293-341. [2] Croft & Soderblom (1991), in *Uranus*, pp. 561-628. [3] Hillier & Squyres (1991), *JGR*, 96, 15665-15674. [4] Pappalardo et al. (1997), *JGR*, 102, 13369-13379. [5] Pappalardo et al. (1998), *Icarus*, 135, 276-302. [6] Prockter et al. (2002), *JGR*, 107, 10.1029/2000JE001458. [7] Pappalardo & Collins (2005), *J. Struct. Geol.*, 27, 827-838. [8] Davis et al. (1983), *JGR*, 88, 1153-1172. [9] Moore (1984), *Icarus*, 59, 205-220. [10] Helfenstein et al. (2006), *LPS* XXXVII, #2182. [11] Beaman et al. (1988), *JGR*, 93, 7625-7633. [12] Durham et al. (1992), *JGR*, 97, 20883-20897. [14] Nimmo (2004), *JGR*, 109, doi:10.1029/2003

JE002168. [13] Dombard & McKinnon (2001), *Icarus*, 154, 321-336. [15] Mueller & McKinnon (1998), *Icarus*, 76, 437-464. [15] Clifford (1993), *JGR*, 98, 10973-11016. [16] Binder & Gunga, *Icarus*, 63, 421-441. [17] Pritchard & Stevenson (2000), in *Origin of the Earth and Moon*, pp. 179-196. [18] Nimmo et al. (2003), *Icarus*, 166, 21-32. [19] Prockter & Pappalardo (2000), *Science*, 289, 941-943. [20] Dombard & McKinnon (2006), *J. Struct. Geol.*, 28, 2259-2269. [21] Davis & Engelder (1985), *Tectonophysics*, 119, 67-88. [22] Goldsby & Kohlstedt (2001), *JGR*, 106, 11017-11030.